Increased CDK1 activity determines the timing of kinetochore-microtubule attachments in meiosis I

Olga Davydenko, Richard M. Schultz, and Michael A. Lampson

Department of Biology, University of Pennsylvania, Philadelphia, PA 19104

Chromosome segregation during cell division depends on stable attachment of kinetochores to spindle microtubules. Mitotic spindle formation and kinetochore–microtubule (K-MT) capture typically occur within minutes of nuclear envelope breakdown. In contrast, during meiosis I in mouse oocytes, formation of the acentrosomal bipolar spindle takes 3–4 h, and stabilization of K-MT attachments is delayed an additional 3–4 h. The mechanism responsible for this delay, which likely prevents stabilization of erroneous attachments during spindle formation, is unknown. Here we show that during meiosis I, attachments are regulated by CDK1 activity, which gradually increases through prometaphase and metaphase I. Partial reduction of CDK1 activity delayed formation of stable attachments, whereas a premature increase in CDK1 activity led to precocious formation of stable attachments and eventually lagging chromosomes at anaphase I. These results indicate that the slow increase in CDK1 activity in meiosis I acts as a timing mechanism to allow stable K-MT attachments only after bipolar spindle formation, thus preventing attachment errors.

Introduction

The goal of the first meiotic division is proper segregation of homologous chromosomes to produce a euploid egg. To achieve faithful segregation at anaphase, the kinetochores of homologous chromosomes must capture microtubules (MTs) emanating from opposite poles of the bipolar spindle (bi-orientation). The two centrosomes of mammalian somatic cells confer an inherent bipolarity to the spindle, such that mitotic spindle formation and kinetochore–MT (K-MT) capture are relatively quick and typically occur within minutes of nuclear envelope breakdown. In contrast, the spindle of the mouse oocyte is acentrosomal and achieves bipolarity through progressive merging of multiple MT organizing centers (MTOCs), first into multipolar intermediates and finally a bipolar spindle 3–4 h after germinal vesicle breakdown (GVBD; Schuh and Ellenberg, 2007). Although chromosomes congress to the equator of this newly formed bipolar spindle, MT fibers do not form stable end-on attachments to kinetochores until late in metaphase I (MI), 6–8 h after GVBD (Brunet et al., 1999; Kitajima et al., 2011; Gui and Homer, 2012).

The mechanism of the attachment delay in meiosis I is unknown, but it may increase the likelihood of bi-orientation by preventing stable attachments while spindles are multipolar and many MTOCs remain close to the chromosomes (Breuer et al., 2010; Kolano et al., 2012; Lane et al., 2012). In cancer cells with multiple centrosomes, attachments that form during a multipolar spindle intermediate can end up incorrect, leading to lagging chromosomes in anaphase and segregation errors (Ganem et al., 2009; Silkworth et al., 2009). A similar problem is likely to arise during meiosis I if attachments are stabilized too soon, before spindle bipolarity is established. Preventing attachment errors may be especially important in oocytes, which can proceed to anaphase I in the presence of misaligned bivalents (Gui and Homer, 2012; Kolano et al., 2012; Lane et al., 2012) and have a high incidence of aneuploidy compared with untransformed somatic cells (Pan et al., 2008; Thompson and Compton, 2008; Chiang et al., 2010).

Although it is unknown how K-MT attachments are delayed in oocytes, the profile of CDK1 activity during meiosis I suggests that this kinase may control the timing. In contrast to mitosis, where CDK1 activity increases rapidly before nuclear

Correspondence to Richard M. Schultz: rschultz@sas.upenn.edu; or Michael A. Lampson: lampson@sas.upenn.edu

The Rockefeller University Press $30.00
J. Cell Biol. Vol. 202 No. 2 221–229
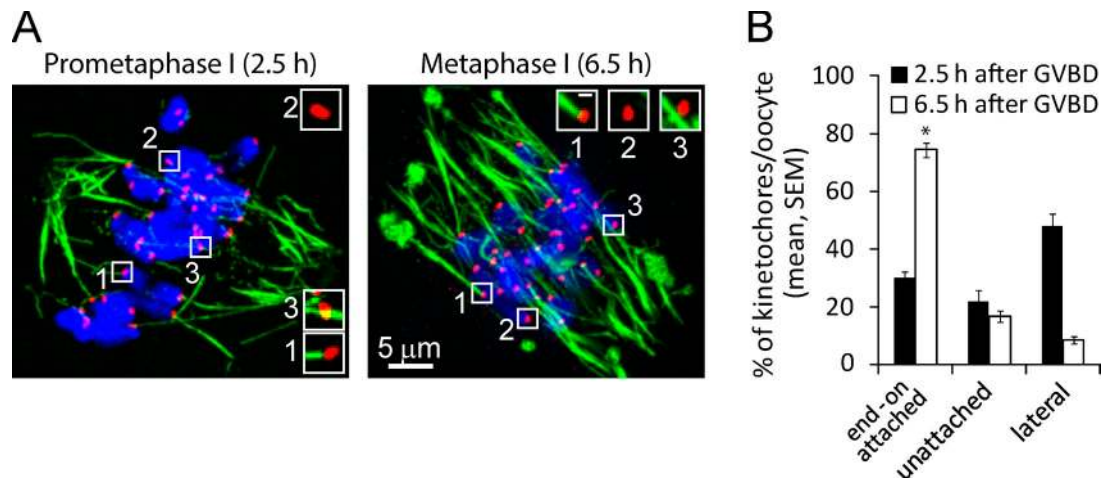www.jcb.org/cgi/doi/10.1083/jcb.201303019

JCB 221

Figure 1. **Stable K-MT attachment is delayed until late in MI.** Oocytes were cultured for 2.5 h after GVBD to prometaphase I or 6.5 h to MI, then analyzed for cold-stable MTs. (A) Images are projections of a confocal z series showing MTs (green), kinetochores (CREST, red), and DNA (blue). Individual kinetochores were classified as end-on attached (1), unattached (2), or lateral (3); insets are optical sections showing examples of each (bar, 0.5 µm). (B) The percent of kinetochores in each category was averaged over multiple cells ($n \geq 17$, 15 kinetochores per cell) at each time point (*, $P < 0.001$).

envelope breakdown and then remains constant until anaphase (Gavet and Pines, 2010), CDK1 activity slowly rises throughout prometaphase and MI in oocytes and peaks ~6 h after GVBD, which is concurrent with stable attachment formation (Choi et al., 1991; Gavin et al., 1994; Polanski et al., 1998). Cyclin B protein progressively accumulates as CDK1 activity increases during meiosis I, which suggests that CDK1 activity is limited by cyclin B levels (Hampl and Eppig, 1995; Winston, 1997). Based on these observations we hypothesize that the gradual increase in cyclin B levels and CDK1 activity act as a timing mechanism to regulate the formation of stable K-MT attachments.

Results and discussion

K-MT attachments are delayed in meiosis I
We first established a cold-stable MT assay to visualize K-MT fibers, which are preferentially stabilized at 4°C while other MTs depolymerize (Rieder, 1981). To quantify K-MT interactions, we scored individual kinetochores as stably end-on attached (contact with ends of cold-stable MTs), unattached (no visible contact to MTs), or lateral (contact with MT, but not end-on; Fig. 1 A). Lateral interaction of kinetochores with MTs typically precedes bi-orientation and attachment stabilization, as chromosomes travel along MTs to congress to the spindle equator (Kapoor et al., 2006; Cai et al., 2009; Magidson et al., 2011). We found that during prometaphase I (2.5 h after GVBD), kinetochores primarily interact laterally with MTs, whereas late in MI (6.5 h after GVBD), ~70% of kinetochores are stably attached (Fig. 1 B). These results are consistent with previous findings (Brunet et al., 1999; Kitajima et al., 2011; Gui and Homer, 2012), and suggest that a timing mechanism controls formation of stable end-on attachments during meiosis I.

Aurora B/C kinases and tension regulate K-MT attachments during meiosis I
Because it is not known how the timing of K-MT interactions is regulated, we tested whether known regulators of K-MT stability function in meiosis I in oocytes. Aurora B kinase, well established as a key regulator, destabilizes attachments by phosphorylating kinetochore proteins responsible for MT binding (Lampson and Cheeseman, 2011). To test this function of Aurora B in meiosis I, oocytes were matured for 5.5 h after GVBD to allow normal spindle formation, then treated with 20 µM ZM447439, an inhibitor of Aurora B and C; Aurora C is a highly similar meiotic isoform. This concentration is the lowest that produces a significant decrease in histone-H3 phosphorylation after a 1-h treatment. We found that Aurora B/C inhibition stabilizes attachments, with nearly 100% of kinetochores connected to cold-stable MT fibers (Fig. 2, A and B). This result shows that during meiosis I, Aurora kinase activity destabilizes K-MT attachments as in mitosis.

Another well-known mechanism contributing to attachment stability is the presence of tension caused by binding of MTs emanating from opposite spindle poles (Nicklas, 1997). Cohesin proteins hold chromosomes together such that tension is generated when MTs pull on kinetochores (Oliveira and Nasmyth, 2010). To test whether tension contributes to stabilizing attachments in oocytes, we prematurely activated separase, the protease responsible for removing cohesins. Two mechanisms independently inhibit separase: phosphorylation by CDK1 and inhibitory binding by securin (Ciosk et al., 1998; Stemmann et al., 2001; Huang et al., 2005). Co-injection of complementary RNA (cRNA) encoding the AA-separase mutant, in which both residues phosphorylated by CDK1 are mutated, together with a securin morpholino, abolishes tension at MI by prematurely destroying chromosome cohesion (Chiang et al., 2011). We find fewer cold-stable attachments in oocytes with separated chromatids, which lack tension, compared with controls with intact cohesion at MI (Fig. 2, C and D). In addition, in the absence of tension, more kinetochores interact with MTs laterally as expected at an earlier stage in spindle formation (Fig. 2 C, insets).

One mechanism by which tension stabilizes attachments is by reducing phosphorylation of Aurora B substrates at kinetochores. To test this relationship between tension and Aurora B/C
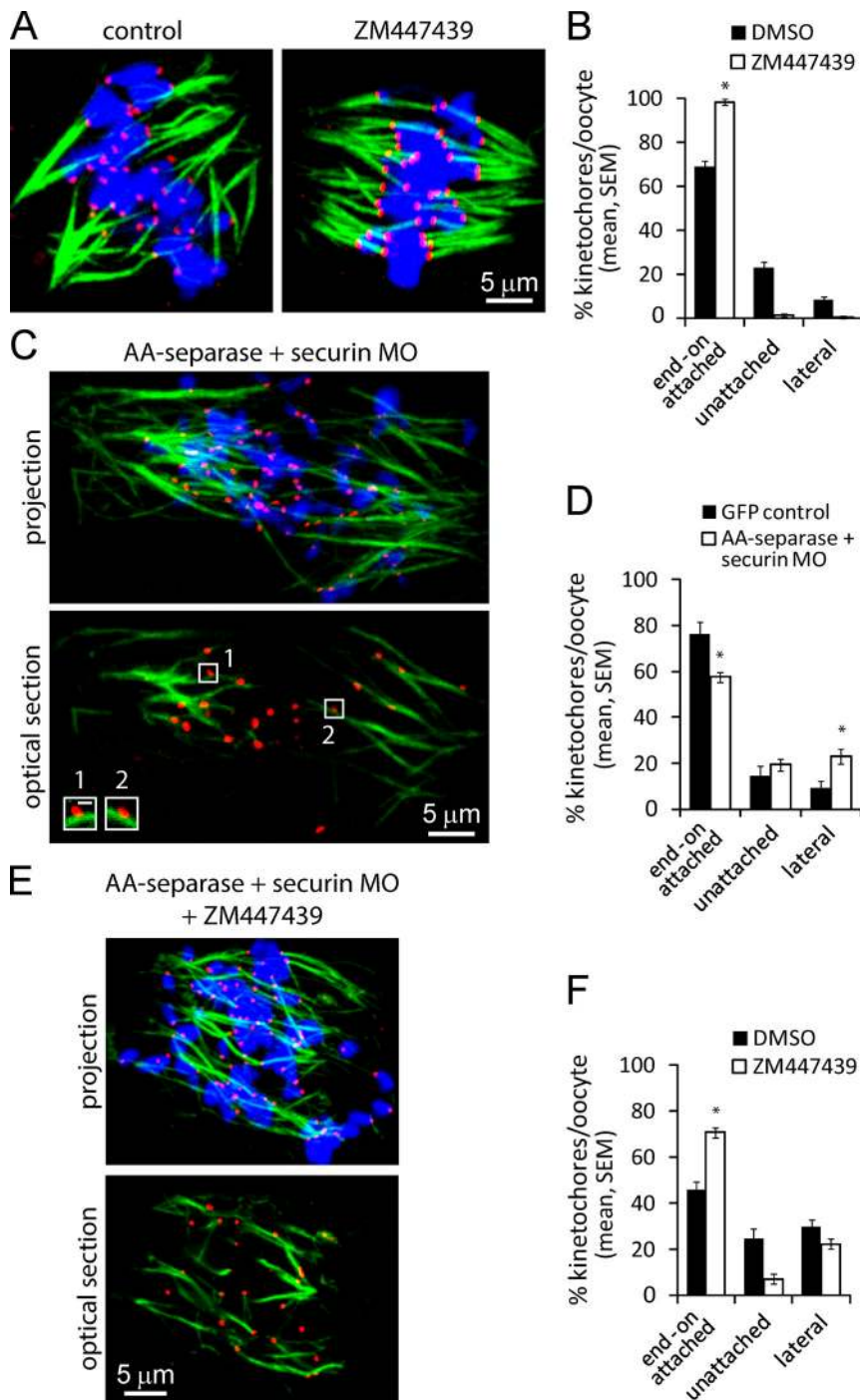
Figure 2. **Aurora B/C kinase activity and tension regulate K-MT attachments during meiosis I.** (A and B) Oocytes were cultured for 5.5 h after GVBD, then treated with Aurora B/C inhibitor ZM447439 or DMSO (control) for 1 h before analysis of cold-stable MTs. (C and D) Oocytes injected with AA-separase cRNA together with securin MO, or GFP cRNA as a control, were matured for 6.5 h after GVBD, then analyzed for cold-stable MTs. (E and F) Oocytes injected with AA-separase cRNA and securin MO were cultured for 5.5 h after GVBD, then treated with ZM447439 (or DMSO) for 1 h before analyzing cold-stable MTs. Only oocytes with complete chromatid separation were analyzed, indicating loss of cohesion. Images (A, C, and E) are projections of a confocal z series showing MTs (green), kinetochores (CREST, red), and DNA (blue). Insets in C are optical sections showing lateral interactions (bar, 0.5 μm). Percentages of end-on attached, unattached, and lateral kinetochores were averaged over multiple cells ($n \geq 13$, ≥ 15 kinetochores per cell; *, $P < 0.001$).

activity during meiosis I, we abolished cohesion while simultaneously inhibiting Aurora B and C. Under these conditions, K-MTs were stabilized to a level similar to that of control oocytes late in MI (Fig. 2, E and F; and Fig. 1 B). These results indicate that established regulators of K-MT attachments, tension and Aurora B/C, likely play a role during meiosis I.

Meiotic CDK1 activity controls the timing of stable K-MT attachments

Although tension and Aurora B/C kinases contribute to regulating attachments in meiosis I, it is not clear how they would explain the timing of stable attachments. To test whether CDK1

activity could act as a timing mechanism, we measured histone H1-kinase activity in vitro with oocytes matured from the germinal vesicle (GV) stage to anaphase I (Fig. S1 A and Fig. 3 A). Histone-H1 kinase activity increases gradually and plateaus 5–6 h after GVBD, when K-MT attachments are stabilized (Fig. 1 B). To test if high CDK1 activity is required to stabilize attachments, we cultured oocytes in low concentrations of the CDK1 inhibitor RO-3306 (0.5 and 2 μM) and followed their progress to anaphase I. These concentrations were chosen to partially inhibit CDK1 activity, as indicated by increased time to GVBD (Fig. 3 B), whereas full inhibition would prevent GVBD. Time from GVBD to chromosome alignment was only

Figure 3. Partial CDK1 inhibition slows stabilization of attachments. (A) Histone-H1 kinase activity was measured in oocytes at the indicated time points relative to GVBD. Each data point represents H1 phosphorylation averaged over three lysates, each with three oocytes. Arrows indicate time of GVBD, anaphase I (AI), and first polar body extrusion (PBE). (B) Oocytes were matured with low concentrations of CDK1 inhibitor RO-3306 (0.5 and 2 µM) or DMSO (control). Meiosis I progression from GV to AI was followed live by DIC microscopy. Times from milrinone washout to GVBD, GVBD to chromosome alignment, and alignment to anaphase I were averaged over multiple cells ($n \geq 18$). (C–F) Oocytes were cultured with 0.5 µM RO-3306 or DMSO for 4.5, 6.5, or 11 h after GVBD, then analyzed for cold-stable MTs. Images in C are projections of a confocal z series or optical sections showing MTs (green) and kinetochores (CREST, red). Insets show individual kinetochores classified as attached (1), unattached (2), or lateral (3); bar, 0.5 µm. Percentages of each attachment state were averaged over multiple cells ($n \geq 23$, 15 kinetochores per cell; *, $P < 0.001$) at each time point.
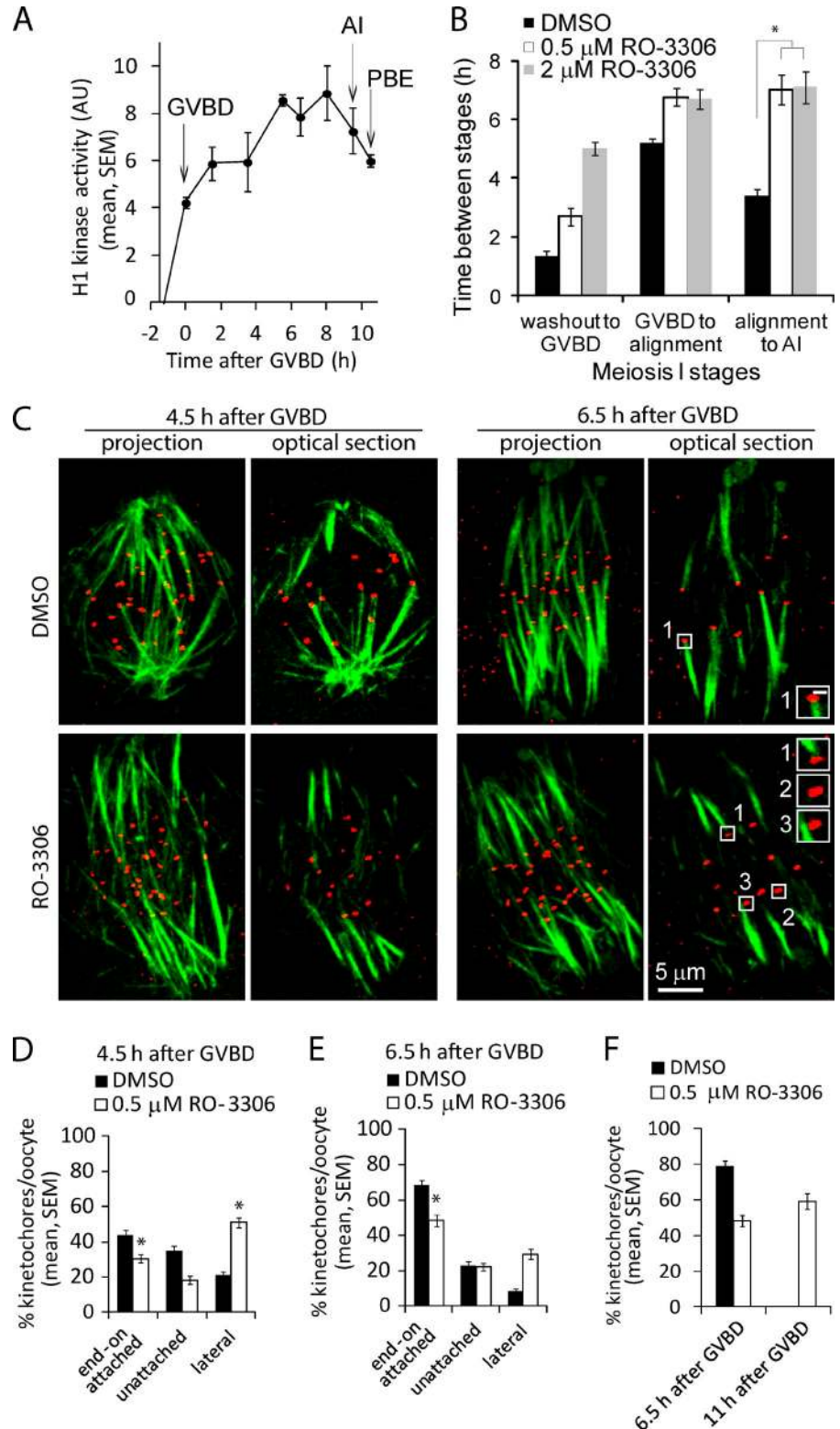
slightly affected by this partial inhibition of CDK1. However after chromosome alignment, the inhibitor-treated cells arrested for >6 h before proceeding to anaphase I, compared with ∼3 h in control oocytes (Fig. 3 B and Fig. S2). Anaphase I onset may be delayed in CDK1-inhibited cells due to a delay in stabilizing K-MT attachments, which would keep the spindle assembly checkpoint (SAC) active longer.

To directly test if partial CDK1 inhibition delays K-MT attachment, we assessed attachments using the cold-stable MT assay. Control oocytes increased their stable attachments from 44% at early MI (4.5 h after GVBD) to 69% late in MI (6.5 h after GVBD). In contrast, CDK1-inhibited oocytes reached only 31% stable attachments at 4.5 h, similar to control oocytes at 2.5 h, and 48% by 6.5 h (Fig. 3, C–E). At 11 h, just before

anaphase I, CDK1-inhibited oocytes still had fewer stable attachments than controls at 6.5 h (Fig. 3 F), which suggests that full CDK1 activity is required to stabilize attachments. In addition, the number of lateral K-MT interactions was consistently higher in oocytes treated with CDK1 inhibitor (Fig. 3, C–E). These results indicate that in oocytes with lower CDK1 activity, kinetochores are more likely to interact with MTs laterally as in earlier stages of spindle formation, and stable end-on binding is delayed.

If the gradual increase in CDK1 activity acts as a timing mechanism to control K-MT interactions, we predict that a more rapid increase would lead to faster K-MT binding. To increase CDK1 activity, we overexpressed cyclin B in oocytes by microinjecting cRNA encoding cyclin B–GFP. We chose this approach because the gradual increase in cyclin B abundance during meiosis I mirrors CDK1 activity levels (Hampl and Eppig, 1995), which suggests that cyclin B limits CDK1 activity. The in vitro histone-H1 kinase assay shows that CDK1 activity increases more rapidly in oocytes overexpressing cyclin B compared with control oocytes (Fig. S1 B and Fig. 4 A). In addition, maximal CDK1 activity is higher in oocytes over-expressing cyclin B. We were unable to find a level of cyclin B overexpression that would result in a similar rapid increase in histone-H1 kinase activity without also increasing the maximal kinase activity. The premature increase in CDK1 activity stabilizes K-MT attachments, with 75% of kinetochores binding cold-stable MTs at 4.5 h after GVBD (early MI), a level similar to control oocytes at late MI (6.5 h after GVBD; Fig. 4, B–D). Consistent with early attachment stabilization, MAD2 disappears from kinetochores by 4.5 h after GVBD in oocytes injected with cyclin B cRNA (Fig. S3, A and B; Waters et al., 1998; Wassmann et al., 2003; Lane et al., 2012). Moreover, prematurely increasing CDK1 activity resulted in stable attachment of nearly all kinetochores at 6.5 h (Fig. 4, B and D). We achieved a similar increase in H1-kinase activity (Fig. S1, C and D) and attachment stabilization by co-injecting a lower amount of cRNA encoding cyclin B together with cRNA encoding CDK1, neither of which on their own increased either H1-kinase activity or attachment stabilization. These results show that we can manipulate K-MT attachments by either reducing or prematurely increasing CDK1 activity.

As potential downstream CDK1 effectors that might contribute to stabilizing K-MTs, we considered TPX2 and hepatoma up-regulated protein (HURP), both of which accumulate on kinetochore fibers during progression through MI (Silljé et al., 2006; Koffa et al., 2006; Wong and Fang, 2006; Brunet et al., 2008; Breuer et al., 2010; Ma et al., 2011). A premature increase in CDK1 activity led to HURP enrichment on kinetochore fibers earlier than in control oocytes (Fig. S3 D), whereas TPX2 localization was not strongly affected (Fig. S3 C). CDK1 activity may directly regulate HURP binding to K-MTs, or the difference in localization may reflect the higher number of stable K-MTs available for HURP to bind.

It may be beneficial for oocytes to delay K-MT stabilization until late in MI to minimize improper attachments in the context of a multipolar spindle. We predicted that early attachment stabilization caused by a premature increase in CDK1 activity
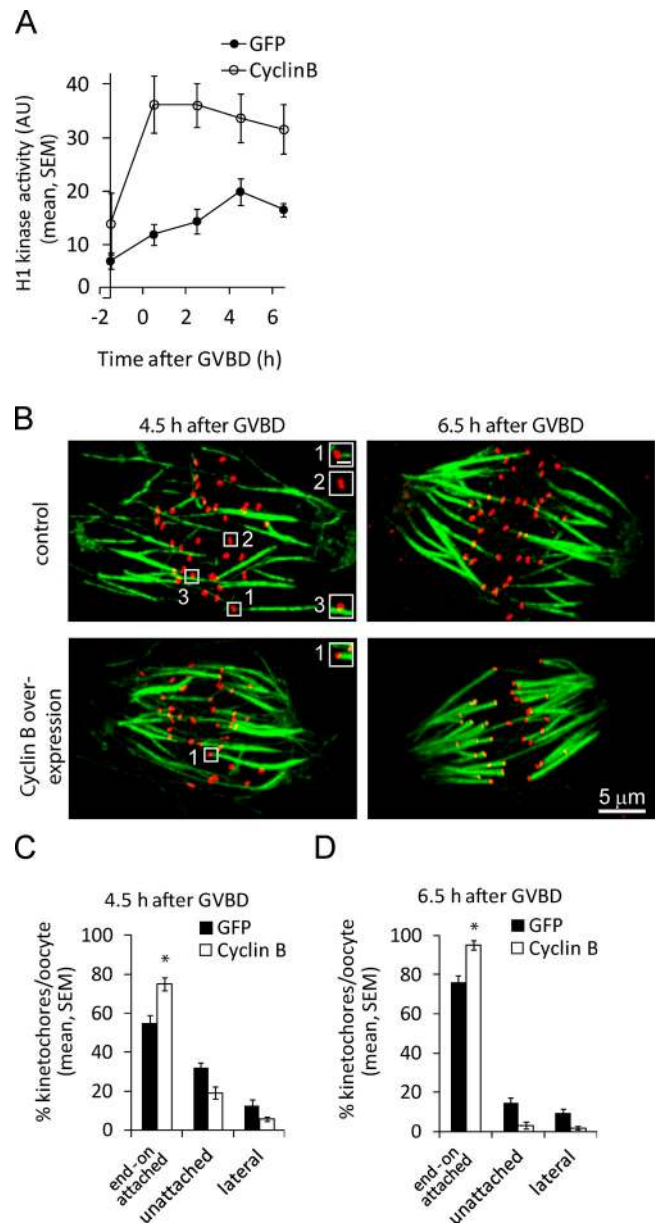

Figure 4. **Prematurely increasing CDK1 activity stabilizes K-MT attachments.** (A and B) Oocytes injected with GFP cRNA or cyclin B–GFP cRNA (700 ng/µl) were analyzed for histone-H1 kinase activity (A) or cold-stable MTs (B) at the indicated time points. H1 kinase activity (A) was averaged over three lysates, each with one oocyte. Images in B are projections of a confocal z series showing MTs (green) and kinetochores (CREST, red). Insets show individual kinetochores classified as attached (1), unattached (2), or lateral (3); bar, 0.5 µm. Injecting lower levels of cyclin B–GFP cRNA (200 ng/µl) together with CDK1 cRNA gave similar results in both the H1 kinase and cold-stable MT assays. (C and D) Percentages of each attachment state were averaged over multiple cells ($n \geq 22$, 15 kinetochores per cell; *, $P < 0.001$) at each time point. Results of the cold-stable MT assay were combined for oocytes injected with cyclin B–GFP cRNA (700 ng/µl) or CDK1 cRNA together with lower levels cyclin B-GFP cRNA (200 ng/µl).

would result in increased incidence of lagging chromosomes at anaphase I as a result of incorrect attachments. We injected oocytes with cRNAs encoding cyclin B to increase CDK1 activity and histone H2B-mCherry to label chromosomes. Levels of cyclin B overexpression that prematurely increase CDK1
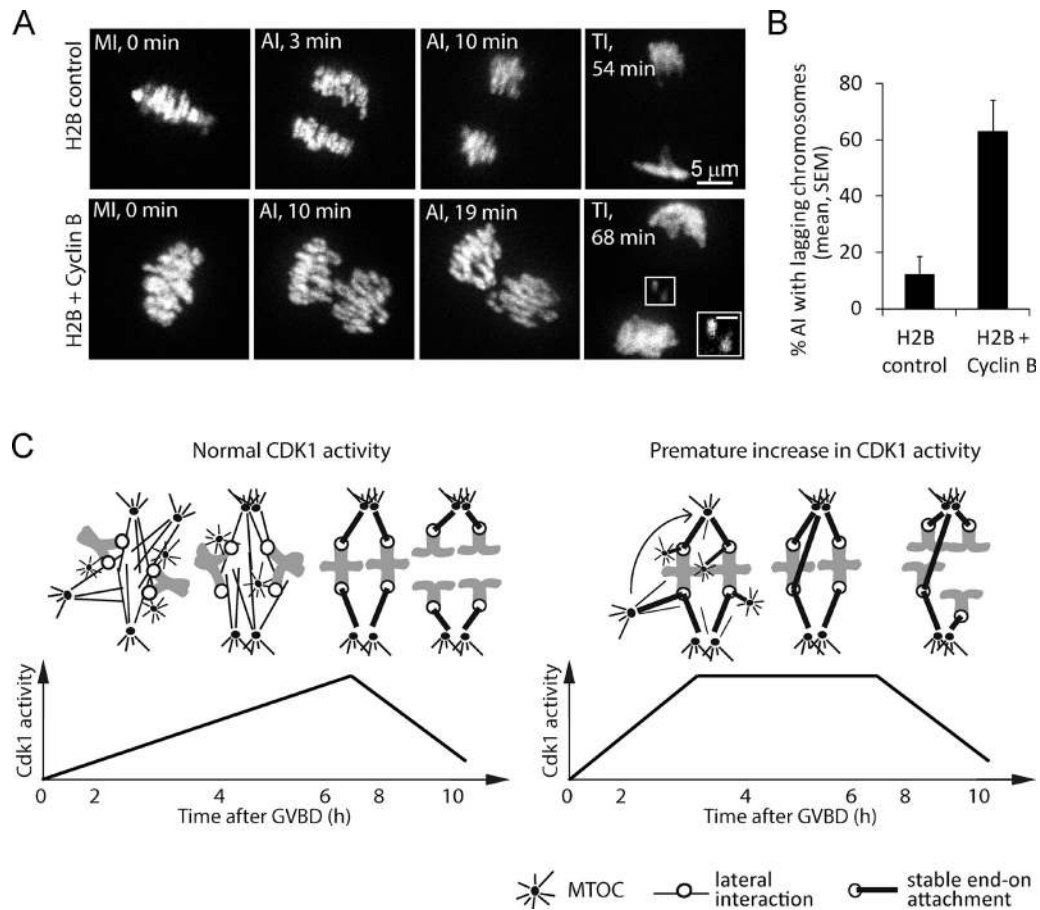
Figure 5. **Prematurely increasing CDK1 activity leads to lagging chromosomes at anaphase I.** (A and B) Oocytes microinjected with H2B-mCherry cRNA, with or without cyclin B–GFP cRNA, were cultured for 6.5 h after GVBD, incubated with 10 µM cycloheximide to allow normal anaphase I progression, and imaged live from MI through telophase I (TI). Images in A are maximal intensity projections of a confocal z series showing all the chromosomes (time stamps relative to anaphase onset). The inset shows lagging chromosomes at anaphase (brightness increased for clarity); bar, 2 µm. The percentage of anaphases with lagging chromosomes was averaged over three independent experiments ($n \geq 5$ cells per experiment; *, P < 0.001). (C) Model schematic depicts the timing of K-MT stabilization when CDK1 activity rises normally (left) vs. prematurely (right) during MI. Normally, kinetochores interact with MTs laterally to achieve chromosome congression, and attachments are stabilized ~7 h after GVBD when CDK1 activity is maximal (left). If K-MT attachments are stabilized too early, in the presence of multipolar spindle intermediates and multiple MTOCs close to the chromosomes, incorrect attachments can lead to lagging chromosomes at anaphase I (right).

activity also arrest oocytes at MI as described previously (Ledan et al., 2001), likely because high cyclin B levels overwhelm the proteasomal degradation machinery. To allow cyclin B degradation, we blocked translation at 6.5 h, when spindle formation is complete in both control and cyclin B–overexpressing oocytes, using the translation inhibitor cycloheximide. Under these conditions, anaphase I occurs with normal timing at 7–10 h after GVBD. We counted lagging chromosomes during anaphase I by live imaging of H2B-mCherry. Anaphases with lagging chromosomes were frequent in oocytes coinjected with cyclin B (63%) compared with control oocytes (12%; Fig. 5), which is consistent with premature stabilization of incorrect attachments early in MI.

Conclusions

We address the question of how the timing of K-MT attachment is regulated during meiosis I in mouse oocytes. We are able to manipulate the timing of K-MT attachments by altering meiotic CDK1 activity: partial CDK1 inhibition delays attachments, and a premature increase in kinase activity stabilizes attachments

early and leads to lagging chromosomes at anaphase I. We conclude that the slow increase in CDK1 activity in meiosis I acts as a timing mechanism to delay stabilization of attachments and prevent segregation errors.

Preventing K-MT stabilization early in MI, in the presence of multipolar spindle intermediates and multiple MTOCs around the chromosomes, serves as a strategy to promote the formation of correctly bi-oriented attachments late in MI (Fig. 5 C). Other mechanisms also increase the likelihood of correct bi-orientation. For example, positioning chromosomes at the spindle equator during prometaphase, through lateral interactions between kinetochores and MTs, promotes kinetochore capture by MTs emanating from opposite spindle poles (Kapoor et al., 2006; Cai et al., 2009; Kitajima et al., 2011; Magidson et al., 2011). This initial chromosome positioning, together with the CDK1-dependent K-MT attachment delay described here, optimizes bi-orientation when stable end-on attachments do form.

Mechanisms that ensure formation of correct attachments are especially important during meiosis I, which is notoriously prone to chromosome segregation errors (Hassold and Hunt, 2009).

The SAC should prevent these errors by delaying anaphase until all chromosomes achieve bi-orientation. Although the SAC is functional in meiosis I (Homer et al., 2005; Niault et al., 2007; Li et al., 2009; McGuinness et al., 2009; Wei et al., 2010; Hached et al., 2011), it is silenced late in MI despite the presence of multiple misaligned chromosomes because these chromosomes do make stable attachments (Gui and Homer, 2012; Kolano et al., 2012; Lane et al., 2012). Our findings suggest that meiosis I is error prone because the SAC is silenced when attachments, whether correct or not, are stabilized by high CDK1 activity late in MI.

In addition to CDK1 activity, other factors may contribute to the timing of attachment stabilization in oocytes. We show here that tension and Aurora B/C kinases contribute to regulation of attachments in MI, and a decrease in Aurora kinase activity or an increase in phosphatase activity may regulate attachment timing. Another potential regulator is the APC/C activator CDH1, as attachments are stabilized early in an oocyte-specific CDH1 knockout (Holt et al., 2012).

The downstream effectors for regulation of K-MT attachments by CDK1 are unknown. As a master regulator of meiosis progression, CDK1 phosphorylates many substrates that play a role in K-MT interactions. For example, CDK1 phosphorylation of the chromosome passenger complex regulates Aurora B localization to centromeres (Tsukahara et al., 2010). Phosphorylation by CDK1 is also required for proper function of MAP-4, an MT-associated protein important for MT stability (Aizawa et al., 1991), and MT plus-end tracking proteins Clip-170 (Yang et al., 2009) and CLASP2 (Maia et al., 2012). In addition, CDK1 phosphorylates known regulators of K-MT interactions such as BubR1 and Mps1 (Jaspersen and Winey, 2004; Wong and Fang, 2007; Morin et al., 2012), and BubR1 phosphorylation recruits B56-PP2A phosphatase to kinetochores, which may stabilize attachments by counteracting Aurora B activity (Kruse et al., 2013). An important goal for future work is to determine which CDK1 targets regulate the timing of K-MT attachments in oocytes.

Materials and methods

Oocyte collection, culture, and microinjection
CF-1 mice (Harlan) were used for all experiments described here. Before oocyte collection, 6–12-wk-old female mice were hormonally primed with equine chorionic gonadotropin (eCG). GV-intact oocytes were collected and microinjected in bicarbonate-free minimal essential medium with polyvinylpyrrolidone and Hepes (MEM-PVP) and cultured in Chatot-Ziomek-Bavister (CZB) medium in an atmosphere of 5% CO_2 in air at 37°C. Meiotic resumption was inhibited by addition of 2.5 µM milrinone (Sigma-Aldrich) or 10 µM RO-3306 (EMD Millipore) in cyclin B–GFP overexpression experiments. Milrinone or RO-3306 were subsequently washed out to allow meiotic resumption. All animal experiments were approved by the institutional animal use and care committee and were consistent with the National Institutes of Health guidelines. The Aurora B/C inhibitor ZM447439 was used at 20 µM and the CDK1 inhibitor RO-3306 at 0.5 or 2 µM.

Oocytes were microinjected in MEM-PVP medium with a micromanipulator (Narishige) and a picoinjector (Medical Systems Corp.); each oocyte was injected with 10 pL. The microinjected oocytes were then incubated for 1 h at 37°C in a humidified atmosphere of 5% CO, in air.

The following cRNAs were used for microinjection: H2B-mCherry (human histone H2B coding sequence with mCherry tag at the C terminus), GFP, or cyclin B–GFP at 700 ng/µl (human cyclin B1 cRNA was generated by amplifying Ccnb1 lacking the first 270 bp, with a GFP tag at the C terminus) generated previously (Schindler and Schultz, 2009). In Fig. 4

(C and D), cyclin B overexpression results were combined with data obtained from coinjection of cRNA encoding CDK1-mCherry with a low level of cRNA encoding cyclin B–GFP (200 ng/µl). The CDK1-mCherry plasmid was generated by inserting the mouse CDC2 into the C-terminal mCherry-pIVT plasmid described previously (Igarashi et al., 2007), and cRNA was synthesized using the TranscriptAid T7 High Yield Transcription kit (Thermo Fisher Scientific). To destroy cohesion at MI, cRNA encoding AA-separase mutant (constructed by mutating both CDK1 phosphorylation sites, S1121A and T1342A) in a full-length mouse separase (Espl1) cDNA clone (Source Bioscience) using the QuikChange Multi Site-Directed Mutagenesis kit, generated previously (Chiang et al., 2011), and securin morpholino (MO) were microinjected into GV-intact oocytes. After microinjection, oocytes were incubated for 16–18 h to allow protein expression.

Cold-stable MT assay and immunocytochemistry
To depolymerize unstable MTs, oocytes were placed in ice-cold MEM-PVP medium for 10 min, followed by fixation and immunocytochemistry. Oocytes were fixed in freshly prepared 2% paraformaldehyde with 0.1% Triton X-100 for 30 min at room temperature, placed in blocking solution (PBS containing 0.3% BSA and 0.01% Tween-20) overnight, then permeabilized in PBS with 0.3% BSA and 0.1% Triton X-100 for 15 min and washed in blocking solution before antibody staining. Human CREST autoimmune serum (1:40 dilution; PerkinElmer) and rabbit β-tubulin (9F3) monoclonal antibody conjugated to Alexa Fluor 488 (1:75 dilution; Cell Signaling Technology) were used to label centromeres and MTs, respectively. After a 1-h incubation with primary antibodies, cells were washed three times, 15 min each wash. The CREST primary antibody was detected using an Alexa Fluor 594–conjugated goat anti–human secondary antibody (Invitrogen). Cells were again washed and mounted in Vectashield with Bisbenzimide Hoechst 33342 (Sigma-Aldrich) to visualize chromosomes.

Confocal images were collected as z stacks at 0.3-µm intervals to visualize the entire meiotic spindle at room temperature using a spinning disc confocal microscope (DMI4000 B; Leica) equipped with a 100× 1.4 NA oil-immersion objective lens, an xy piezo Z stage (Applied Scientific Instrumentation), a spinning disk confocal scanner (Yokogawa Corporation of America), an electron multiplier charge-coupled device camera (ImageEM C9100-13; Hamamatsu Photonics), and an LMM5 laser merge module with 488- and 593-nm diode lasers (Spectral Applied Research) controlled by MetaMorph software (Molecular Devices). The Subtract Background tool of ImageJ (National Institutes of Health) with 20 pixel radius was used for image presentation. To classify kinetochore attachments, the CREST channel was used to select a centromere while blind to MTs, then its attachment status was scored around the same z plane using the merged two-color confocal stack of CREST and MT images.

MAD2, HURP, and TPX2 were stained using the immunocytochemistry protocol described earlier in this section. The rabbit polyclonal antibody raised against human MAD2 (Kops et al., 2005), a gift from B. Weaver (University of Wisconsin-Madison, Madison, WI), was used at 1:200 dilution. To quantify MAD2 levels at kinetochores, MAD2 intensity was measured only where it colocalized with CREST and normalized by the CREST signal intensity for every cell. The rabbit immune serum raised against the human TPX2 (Brunet et al., 2008), a gift from O. Gruss (Zentrum für Molekulare Biologie der Universität Heidelberg, Heidelberg, Germany), was used at 1:500 dilution. The rabbit polyclonal antibody raised against mouse HURP (Santa Cruz Biotechnology, Inc.) was used at 1:200 dilution.

Histone-H1 kinase assay
Oocytes were collected and cultured as described in the "Oocyte collection, culture, and microinjection" section for the amount of time indicated then immediately frozen in kinase lysis buffer. The histone-H1 kinase reaction was initiated by the addition of 5 µl of kinase buffer (24 mM p-nitrophenyl phosphate, 90 mM β-glycerophosphate, 24 mM $MgCl_2$, 24 mM EGTA, 0.2 mM EDTA, 4.6 mM sodium orthovanadate, 4 mM NaF, 1.6 mM dithiothreitol, 60 µg/ml aprotinin, 60 µg/ml leupeptin, 2 mg/ml polyvinyl alcohol, 2.2 µM protein kinase A inhibitor peptide [Sigma-Aldrich], 40 mM MOPS, pH 7.2, 0.6 mM ATP, and 2 mg/ml histone [type III-S; Sigma-Aldrich]) with 500 µCi/ml γ-[^{32}P]ATP (3,000 Ci/mmol; GE Healthcare). To determine the background level of phosphorylation for histone-H1, 5 µl of double kinase lysis buffer was added instead of oocyte lysate. The reaction was conducted for 30 min at 30°C and terminated by the addition of 10 µl of double-strength concentrated SDS-PAGE sample buffer and boiling for 3 min. After SDS-PAGE, the 15% gel was fixed in 10% acetic acid/30% methanol, dried, and exposed to a PhosphoImager screen for 16 to 24 h. Gel images were detected on a Typhoon 9410 PhosphoImager

(GE Healthcare), and band intensities were quantified using ImageJ software (National Institutes of Health). CDK1 activity was assessed by the phosphorylation status of histone-H1 based on the PhosphoImager gel results. Control lanes (lysis buffer with no lysate) were used for background subtraction. Representative experiments are shown and were repeated with similar results.

Live differential interference contrast (DIC) and confocal imaging

To measure the timing of meiotic progression after partial CDK1 inhibition, oocytes were washed out of milrinone into CZB medium containing DMSO (1:1,000) or 0.5 or 2 µM RO-3306 to allow GVBD but partially inhibit CDK1 activity. The oocytes were then placed in the same medium in a glass-bottom dish coated with protamine sulfate (Sigma-Aldrich) as described previously (Bornslaeger et al., 1986), which allows oocytes to attach to the glass. DIC images were acquired using a microscope (DMI6000 B; Leica) equipped with a 40× 1.25 NA oil-immersion objective, a charge-coupled device camera (QuantEM, 512 SC; Photometrics) controlled by MetaMorph software, and a stage top incubator (ZILCS; Tokai Hit) heated at 37°C with 5% CO_2. Oocytes were imaged by DIC from GVBD until anaphase I every 12 min as z stacks at 5-µm intervals to monitor time to GVBD, chromosome alignment, and polar body extrusion. Chromosome alignment was defined as the first time when no misaligned chromosomes were apparent by DIC in any of the z planes.

To follow anaphase I progression live, oocytes were injected with cRNA encoding H2B-mCherry and cyclin B to increase CDK1 activity and label chromosomes, then incubated for 16–18 h to allow protein expression in 10 µM RO-3306. Because CDK1 activity was increased in these oocytes due to cyclin B overexpression, a CDK1 inhibitor was used to prevent spontaneous GVBD. At 6.5 h after GVBD, oocytes were placed in 10 µM cycloheximide to inhibit further cyclin B protein expression and allow anaphase I to progress normally. Oocytes were then placed in protamine sulfate–coated dishes and into a heated environmental chamber (Incubator BL; PeCon GmBH) with a stage top incubator (DM IRB+IRE2) to maintain 5% CO_2 in air and 37°C. Confocal images of H2B-mCherry were acquired every 3 min using the spinning disc confocal microscope described above with a 63× 1.4 NA glycerol-immersion objective lens. Images were acquired as z stacks at 1-µm intervals capturing all the chromosomes.

Online supplemental material

Fig. S1 shows representative histone-H1 kinase assays quantified in Figs. 3 A and 4 A. Fig. S2 shows representative DIC images of meiotic progression, as quantified in Fig. 3 B. Fig. S3 shows Mad2, HURP, and TPX2 staining in controls and oocytes injected with cyclin B cRNA. Online supplemental material is available at http://www.jcb.org/cgi/content/full/jcb.201303019/DC1.

References

Aizawa, H., M. Kamijo, Y. Ohba, A. Mori, K. Okuhara, H. Kawasaki, H. Murofushi, K. Suzuki, and H. Yasuda. 1991. Microtubule destabilization by cdc2/H1 histone kinase: phosphorylation of a "pro-rich region" in the microtubule-binding domain of MAP-4. *Biochem. Biophys. Res. Commun.* 179:1620–1626. http://dx.doi.org/10.1016/0006-291X(91)91760-A

Bornslaeger, E.A., P. Mattei, and R.M. Schultz. 1986. Involvement of cAMP-dependent protein kinase and protein phosphorylation in regulation of mouse oocyte maturation. *Dev. Biol.* 114:453–462. http://dx.doi.org/10.1016/0012-1606(86)90209-5

Breuer, M., A. Kolano, M. Kwon, C.-C. Li, T.-F. Tsai, D. Pellman, S. Brunet, and M.-H. Verlhac. 2010. HURP permits MTOC sorting for robust meiotic spindle bipolarity, similar to extra centrosome clustering in cancer cells. *J. Cell Biol.* 191:1251–1260. http://dx.doi.org/10.1083/jcb.201005065

Brunet, S., A.S. Maria, P. Guillaud, D. Dujardin, J.Z. Kubiak, and B. Maro. 1999. Kinetochore fibers are not involved in the formation of the first meiotic spindle in mouse oocytes, but control the exit from the first meiotic M phase. *J. Cell Biol.* 146:1–12. http://dx.doi.org/10.1083/jcb.146.1.1

Brunet, S., J. Dumont, K.W. Lee, K. Kinoshita, P. Hikal, O.J. Gruss, B. Maro, and M.-H. Verlhac. 2008. Meiotic regulation of TPX2 protein levels governs cell cycle progression in mouse oocytes. *PLoS ONE.* 3:e3338. http://dx.doi.org/10.1371/journal.pone.0003338

Cai, S., C.B. O'Connell, A. Khodjakov, and C.E. Walczak. 2009. Chromosome congression in the absence of kinetochore fibres. *Nat. Cell Biol.* 11:832–838. http://dx.doi.org/10.1038/ncb1890

Chiang, T., F.E. Duncan, K. Schindler, R.M. Schultz, and M.A. Lampson. 2010. Evidence that weakened centromere cohesion is a leading cause of age-related aneuploidy in oocytes. *Curr. Biol.* 20:1522–1528. http://dx.doi.org/10.1016/j.cub.2010.06.069

Chiang, T., R.M. Schultz, and M.A. Lampson. 2011. Age-dependent susceptibility of chromosome cohesion to premature separase activation in mouse oocytes. *Biol. Reprod.* 85:1279–1283. http://dx.doi.org/10.1095/biolreprod.111.094094

Choi, T., F. Aoki, M. Mori, M. Yamashita, Y. Nagahama, and K. Kohmoto. 1991. Activation of p34cdc2 protein kinase activity in meiotic and mitotic cell cycles in mouse oocytes and embryos. *Development.* 113:789–795.

Ciosk, R., W. Zachariae, C. Michaelis, A. Shevchenko, M. Mann, and K. Nasmyth. 1998. An ESP1/PDS1 complex regulates loss of sister chromatid cohesion at the metaphase to anaphase transition in yeast. *Cell.* 93:1067–1076. http://dx.doi.org/10.1016/S0092-8674(00)81211-8

Ganem, N.J., S.A. Godinho, and D. Pellman. 2009. A mechanism linking extra centrosomes to chromosomal instability. *Nature.* 460:278–282. http://dx.doi.org/10.1038/nature08136

Gavet, O., and J. Pines. 2010. Progressive activation of CyclinB1-Cdk1 coordinates entry to mitosis. *Dev. Cell.* 18:533–543. http://dx.doi.org/10.1016/j.devcel.2010.02.013

Gavin, A.C., J.C. Cavadore, and S. Schorderet-Slatkine. 1994. Histone H1 kinase activity, germinal vesicle breakdown and M phase entry in mouse oocytes. *J. Cell Sci.* 107:275–283.

Gui, L., and H. Homer. 2012. Spindle assembly checkpoint signalling is uncoupled from chromosomal position in mouse oocytes. *Development.* 139:1941–1946. http://dx.doi.org/10.1242/dev.078352

Hached, K., S.Z. Xie, E. Buffin, D. Cladière, C. Rachez, M. Sacras, P.K. Sorger, and K. Wassmann. 2011. Mps1 at kinetochores is essential for female mouse meiosis I. *Development.* 138:2261–2271. http://dx.doi.org/10.1242/dev.061317

Hampl, A., and J.J. Eppig. 1995. Translational regulation of the gradual increase in histone H1 kinase activity in maturing mouse oocytes. *Mol. Reprod. Dev.* 40:9–15. http://dx.doi.org/10.1002/mrd.1080400103

Hassold, T., and P. Hunt. 2009. Maternal age and chromosomally abnormal pregnancies: what we know and what we wish we knew. *Curr. Opin. Pediatr.* 21:703–708. http://dx.doi.org/10.1097/MOP.0b013e328332c6ab

Holt, J.E., S.I.R. Lane, P. Jennings, I. García-Higuera, S. Moreno, and K.T. Jones. 2012. APC(FZR1) prevents nondisjunction in mouse oocytes by controlling meiotic spindle assembly timing. *Mol. Biol. Cell.* 23:3970–3981. http://dx.doi.org/10.1091/mbc.E12-05-0352

Homer, H.A., A. McDougall, M. Levasseur, A.P. Murdoch, and M. Herbert. 2005. Mad2 is required for inhibiting securin and cyclin B degradation following spindle depolymerisation in meiosis I mouse oocytes. *Reproduction.* 130:829–843. http://dx.doi.org/10.1530/rep.1.00856

Huang, X., R. Hatcher, J.P. York, and P. Zhang. 2005. Securin and separase phosphorylation act redundantly to maintain sister chromatid cohesion in mammalian cells. *Mol. Biol. Cell.* 16:4725–4732. http://dx.doi.org/10.1091/mbc.E05-03-0190

Igarashi, H., J.G. Knott, R.M. Schultz, and C.J. Williams. 2007. Alterations of PLCbeta1 in mouse eggs change calcium oscillatory behavior following fertilization. *Dev. Biol.* 312:321–330. http://dx.doi.org/10.1016/j.ydbio.2007.09.028

Jaspersen, S.L., and M. Winey. 2004. The budding yeast spindle pole body: structure, duplication, and function. *Annu. Rev. Cell Dev. Biol.* 20:1–28. http://dx.doi.org/10.1146/annurev.cellbio.20.022003.114106

Kapoor, T.M., M.A. Lampson, P. Hergert, L. Cameron, D. Cimini, E.D. Salmon, B.F. McEwen, and A. Khodjakov. 2006. Chromosomes can congress to the metaphase plate before biorientation. *Science.* 311:388–391. http://dx.doi.org/10.1126/science.1122142

Kitajima, T.S., M. Ohsugi, and J. Ellenberg. 2011. Complete kinetochore tracking reveals error-prone homologous chromosome biorientation in mammalian oocytes. *Cell.* 146:568–581. http://dx.doi.org/10.1016/j.cell.2011.07.031

Koffa, M.D., C.M. Casanova, R. Santarella, T. Köcher, M. Wilm, and I.W. Mattaj. 2006. HURP is part of a Ran-dependent complex involved in spindle formation. *Curr. Biol.* 16:743–754. http://dx.doi.org/10.1016/j.cub.2006.03.056

Kolano, A., S. Brunet, A.D. Silk, D.W. Cleveland, and M.H. Verlhac. 2012. Error-prone mammalian female meiosis from silencing the spindle

assembly checkpoint without normal interkinetochore tension. *Proc. Natl. Acad. Sci. USA*. 109:E1858–E1867. http://dx.doi.org/10.1073/pnas .1204686109

Kops, G.J.P.L., Y. Kim, B.A. Weaver, Y. Mao, I. McLeod, J.R. Yates III, M. Tagaya, and D.W. Cleveland. 2005. ZW10 links mitotic checkpoint signaling to the structural kinetochore. *J. Cell Biol.* 169:49–60. http://dx .doi.org/10.1083/jcb.200411118

Kruse, T., G. Zhang, M.S.Y. Larsen, T. Lischetti, W. Streicher, T. Kragh Nielsen, S.P. Bjørn, and J. Nilsson. 2013. Direct binding between BubR1 and B56-PP2A phosphatase complexes regulate mitotic progression. *J. Cell Sci.* 126:1086–1092. http://dx.doi.org/10.1242/jcs.122481

Lampson, M.A., and I.M. Cheeseman. 2011. Sensing centromere tension: Aurora B and the regulation of kinetochore function. *Trends Cell Biol.* 21:133–140. http://dx.doi.org/10.1016/j.tcb.2010.10.007

Lane, S.I., Y. Yun, and K.T. Jones. 2012. Timing of anaphase-promoting complex activation in mouse oocytes is predicted by microtubule-kinetochore attachment but not by bivalent alignment or tension. *Development*. 139:1947–1955. http://dx.doi.org/10.1242/dev.077040

Ledan, E., Z. Polanski, M.E. Terret, and B. Maro. 2001. Meiotic maturation of the mouse oocyte requires an equilibrium between cyclin B synthesis and degradation. *Dev. Biol.* 232:400–413. http://dx.doi.org/10.1006/dbio .2001.0188

Li, M., S. Li, J. Yuan, Z.-B. Wang, S.-C. Sun, H. Schatten, and Q.-Y. Sun. 2009. Bub3 is a spindle assembly checkpoint protein regulating chromosome segregation during mouse oocyte meiosis. *PLoS ONE*. 4:e7701. http:// dx.doi.org/10.1371/journal.pone.0007701

Ma, N., J. Titus, A. Gable, J.L. Ross, and P. Wadsworth. 2011. TPX2 regulates the localization and activity of Eg5 in the mammalian mitotic spindle. *J. Cell Biol.* 195:87–98. http://dx.doi.org/10.1083/jcb.201106149

Magidson, V., C.B. O'Connell, J. Lončarek, R. Paul, A. Mogilner, and A. Khodjakov. 2011. The spatial arrangement of chromosomes during prometaphase facilitates spindle assembly. *Cell*. 146:555–567. http://dx.doi .org/10.1016/j.cell.2011.07.012

Maia, A.R.R., Z. Garcia, L. Kabeche, M. Barisic, S. Maffini, S. Macedo-Ribeiro, I.M. Cheeseman, D.A. Compton, I. Kaverina, and H. Maiato. 2012. Cdk1 and Plk1 mediate a CLASP2 phospho-switch that stabilizes kinetochore-microtubule attachments. *J. Cell Biol.* 199:285–301. http://dx.doi.org/ 10.1083/jcb.201203091

McGuinness, B.E., M. Anger, A. Kouznetsova, A.M. Gil-Bernabé, W. Helmhart, N.R. Kudo, A. Wuensche, S. Taylor, C. Hoog, B. Novak, and K. Nasmyth. 2009. Regulation of APC/C activity in oocytes by a Bub1-dependent spindle assembly checkpoint. *Curr. Biol.* 19:369–380. http://dx.doi.org/ 10.1016/j.cub.2009.01.064

Morin, V., S. Prieto, S. Melines, S. Hem, M. Rossignol, T. Lorca, J. Espeut, N. Morin, and A. Abrieu. 2012. CDK-dependent potentiation of MPS1 kinase activity is essential to the mitotic checkpoint. *Curr. Biol.* 22:289–295. http://dx.doi.org/10.1016/j.cub.2011.12.048

Niault, T., K. Hached, R. Sotillo, P.K. Sorger, B. Maro, R. Benezra, and K. Wassmann. 2007. Changing Mad2 levels affects chromosome segregation and spindle assembly checkpoint control in female mouse meiosis I. *PLoS ONE*. 2:e1165. http://dx.doi.org/10.1371/journal.pone.0001165

Nicklas, R.B. 1997. How cells get the right chromosomes. *Science*. 275:632–637. http://dx.doi.org/10.1126/science.275.5300.632

Oliveira, R.A., and K. Nasmyth. 2010. Getting through anaphase: splitting the sisters and beyond. *Biochem. Soc. Trans*. 38:1639–1644. http://dx.doi .org/10.1042/BST0381639

Pan, H., P. Ma, W. Zhu, and R.M. Schultz. 2008. Age-associated increase in aneuploidy and changes in gene expression in mouse eggs. *Dev. Biol.* 316:397–407. http://dx.doi.org/10.1016/j.ydbio.2008.01.048

Polanski, Z., E. Ledan, S. Brunet, S. Louvet, M.H. Verlhac, J.Z. Kubiak, and B. Maro. 1998. Cyclin synthesis controls the progression of meiotic maturation in mouse oocytes. *Development*. 125:4989–4997.

Rieder, C.L. 1981. The structure of the cold-stable kinetochore fiber in metaphase PtK1 cells. *Chromosoma*. 84:145–158. http://dx.doi.org/10.1007/ BF00293368

Schindler, K., and R.M. Schultz. 2009. CDC14B acts through FZR1 (CDH1) to prevent meiotic maturation of mouse oocytes. *Biol. Reprod.* 80:795–803. http://dx.doi.org/10.1095/biolreprod.108.074906

Schuh, M., and J. Ellenberg. 2007. Self-organization of MTOCs replaces centrosome function during acentrosomal spindle assembly in live mouse oocytes. *Cell*. 130:484–498. http://dx.doi.org/10.1016/j.cell.2007.06.025

Silkworth, W.T., I.K. Nardi, L.M. Scholl, and D. Cimini. 2009. Multipolar spindle pole coalescence is a major source of kinetochore mis-attachment and chromosome mis-segregation in cancer cells. *PLoS ONE*. 4:e6564. http:// dx.doi.org/10.1371/journal.pone.0006564

Silljé, H.H.W., S. Nagel, R. Körner, and E.A. Nigg. 2006. HURP is a Ran-importin beta-regulated protein that stabilizes kinetochore microtubules

in the vicinity of chromosomes. *Curr. Biol.* 16:731–742. http://dx.doi .org/10.1016/j.cub.2006.02.070

Stemmann, O., H. Zou, S.A. Gerber, S.P. Gygi, and M.W. Kirschner. 2001. Dual inhibition of sister chromatid separation at metaphase. *Cell*. 107:715–726. http://dx.doi.org/10.1016/S0092-8674(01)00603-1

Thompson, S.L., and D.A. Compton. 2008. Examining the link between chromosomal instability and aneuploidy in human cells. *J. Cell Biol.* 180:665–672. http://dx.doi.org/10.1083/jcb.200712029

Tsukahara, T., Y. Tanno, and Y. Watanabe. 2010. Phosphorylation of the CPC by Cdk1 promotes chromosome bi-orientation. *Nature*. 467:719–723. http://dx.doi.org/10.1038/nature09390

Wassmann, K., T. Niault, and B. Maro. 2003. Metaphase I arrest upon activation of the Mad2-dependent spindle checkpoint in mouse oocytes. *Curr. Biol.* 13:1596–1608. http://dx.doi.org/10.1016/j.cub.2003.08.052

Waters, J.C., R.H. Chen, A.W. Murray, and E.D. Salmon. 1998. Localization of Mad2 to kinetochores depends on microtubule attachment, not tension. *J. Cell Biol.* 141:1181–1191. http://dx.doi.org/10.1083/jcb.141.5.1181

Wei, L., X.-W. Liang, Q.-H. Zhang, M. Li, J. Yuan, S. Li, S.-C. Sun, Y.-C. Ouyang, H. Schatten, and Q.-Y. Sun. 2010. BubR1 is a spindle assembly checkpoint protein regulating meiotic cell cycle progression of mouse oocyte. *Cell Cycle*. 9:1112–1121. http://dx.doi.org/10.4161/cc.9.6.10957

Winston, N.J. 1997. Stability of cyclin B protein during meiotic maturation and the first mitotic cell division in mouse oocytes. *Biol. Cell*. 89:211–219.

Wong, J., and G. Fang. 2006. HURP controls spindle dynamics to promote proper interkinetochore tension and efficient kinetochore capture. *J. Cell Biol.* 173:879–891. http://dx.doi.org/10.1083/jcb.200511132

Wong, O.K., and G. Fang. 2007. Cdk1 phosphorylation of BubR1 controls spindle checkpoint arrest and Plk1-mediated formation of the 3F3/2 epitope. *J. Cell Biol.* 179:611–617. http://dx.doi.org/10.1083/jcb.200708044

Yang, X., H. Li, X.S. Liu, A. Deng, and X. Liu. 2009. Cdc2-mediated phosphorylation of CLIP-170 is essential for its inhibition of centrosome reduplication. *J. Biol. Chem.* 284:28775–28782. http://dx.doi.org/10.1074/jbc .M109.017681